DETERMINATION OF ELECTROCHEMICAL PERFORMANCE, AND THERMO-MECHANICAL-CHEMICAL STABILITY OF SOFCS FROM DEFECT MODELING

Eric D. Wachsman and Keith L. Duncan
Department of Materials Science
University of Florida, Gainesville FL 32611

OBJECTIVES

1. Provide fundamental relationships between SOFC performance and operating conditions (T, P_{O_2}, V, etc..)

2. Transient (time dependent) transport properties

3. Extend models to:
   - Thermo-mechanical stability
     - Thermal and thermochemical expansion
     - Elastic modulus
     - Fracture toughness
   - Thermo-chemical stability
     - Pore formation and reactions at cathode/electrolyte interface
   - Multilayer structures
     - Interfacial defect concentration, etc.

4. Incorporate microstructural effects such as grain boundaries and grain-size distribution

5. Experimentally verify models and devise strategies to obtain relevant material constants

6. Assemble software package for integration into SECA failure analysis models

TASKS PERFORMED IN PHASE 1

1. Completed continuum-level electrochemical model (CLEM) with a non-linear Galvani potential and potential-dependent boundary values.

2. Extended CLEM to thermo-chemical and thermo-mechanical properties.

3. Modeled transient behavior of defects in SOFCs.

4. Experimentally determined SOFC related time constants from R-C circuit analysis of cathodes, electrolytes and anodes for evaluating the effect of voltage transients from the power conditioning equipment on failure mechanisms and other time dependent properties. These will be integrated into the model in Phase II.

5. Developed a software package for CLEM to integrate into SOFC performance models used by NETL, PNNL, ORNL and the SECA industrial teams.

TASKS TO BE PERFORMED IN PHASE II

1. Extend Continuum-Level Electrochemical Model to Include Multi-Layer Structures
    Determine effects of component thickness ratios and operating conditions on the concentration of defect species and oxygen potential at component interfaces.

2. Extend Continuum-Level Electrochemical Model to Include Microstructural Effects
    Determine effects of microstructure on the electrical, thermo-mechanical and thermo-chemical stability of SOFC components and SOFC performance.

3. Experimentally Verify Thermo-Mechanical Model
    Measure oxygen stoichiometry (Cahn Microbalance) and material expansion (Theta Dilatometer) as a function of P_{O_2} & T. Measure modulus and fracture toughness of single crystal regions as a function of P_{O_2} & T (Triboindenter). Measure modulus and fracture toughness of polycrystalline samples (MTS system) and separate bulk property vs. microstructural effects. Compare with data obtained at ORNL.

4. Verify Electrochemical Performance , Chemical Stability, and Transient Aspects of Model
    Obtain frequency dependent impedance and electrode overpotential data from electrochemical measurements (ac impedance spectroscopy, potentiometric, current interrupt, etc,) to determine effects of porosity and pore diffusion (electrodes); grain boundaries (electrolyte); and grain-size distribution.
    Induce degradation/failure in cathode/electrolyte bilayers by thermal cycling, high temperature sintering and DC bias to initiate tertiary phase formation or delamination at the interface. Experimentally determine cell time constants from R-C circuit analysis and use in evaluating the effect of voltage transients from the power conditioning equipment on failure mechanisms.

5. Package and Deliver Software
    Develop software modules of the models for use by NETL, PNNL, ORNL and SECA industrial teams.

Features of the Defect Model

• Continuous functions for the defect concentrations vs. discontinuous "piecewise" Brouwer approach.

• Dependent on thermodynamic quantities, namely the mass-action constants (K's).

• Quantitative for any SOE/MIEC.

• Derived from fundamental thermodynamic equations.

Electron-Hole Pair Formation

$$null \leftrightarrow e' + h^{\bullet}$$

$$K_i = c_e c_h = N_v N_c \exp\left(-E_g / k_B T\right)$$

External Equilibria

$$O_O^{\times} \leftrightarrow V_O^{\bullet\bullet} + 2e' + \tfrac{1}{2} O_2$$
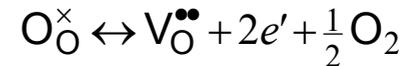
$$K_r = c_V c_e^2 P_{O_2}^{\frac{1}{2}} = K_r^* \exp\left(-\Delta G_r / k_B T\right)$$

Internal Equilibria

$$O_O^{\times} \leftrightarrow V_O^{\bullet\bullet} + O_I''$$
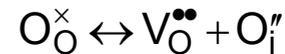
$$K_f = c_V c_I$$

Defect Triads   **vs.**   **Defect Pairs**
(CLEM)   **(Brouwer)**

$$c_e + c_A = 2c_V$$

Limiting Case

$$P_{O_2} \gg 4^{-4} K_r^2 c_V^{-6}$$

$$c_e = 2c_V \quad \text{...Region I}$$

$$c_A = 2c_V \quad \text{...Region IIa}$$

CONTINUUM LEVEL ELECTROCHEMICAL MODEL - Defect Equilibria

FLUORITE
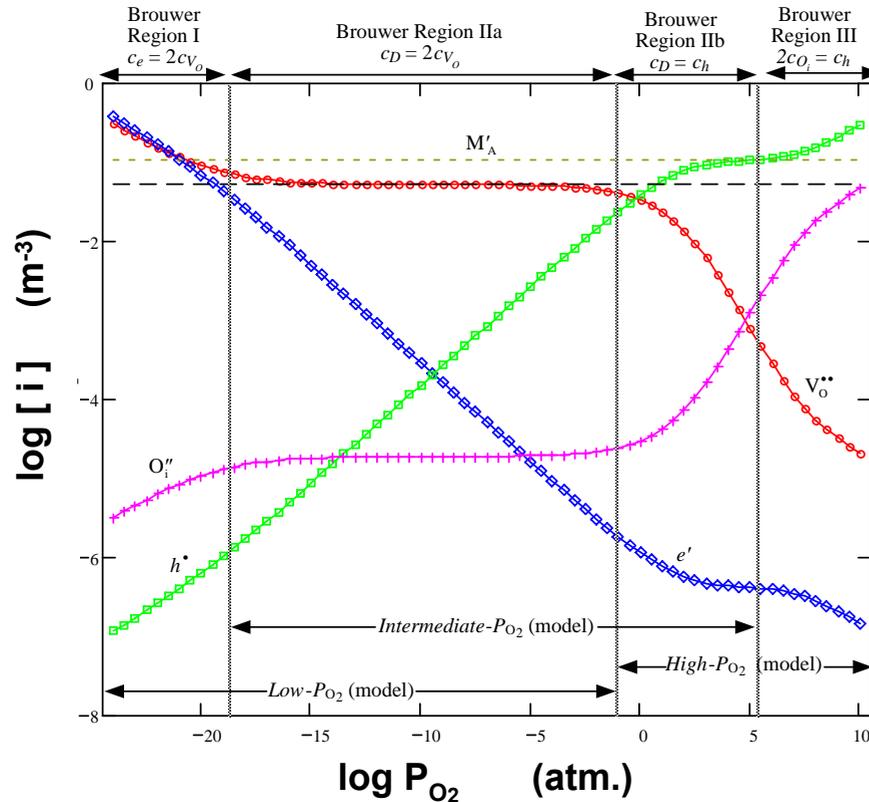
PEROVSKITE
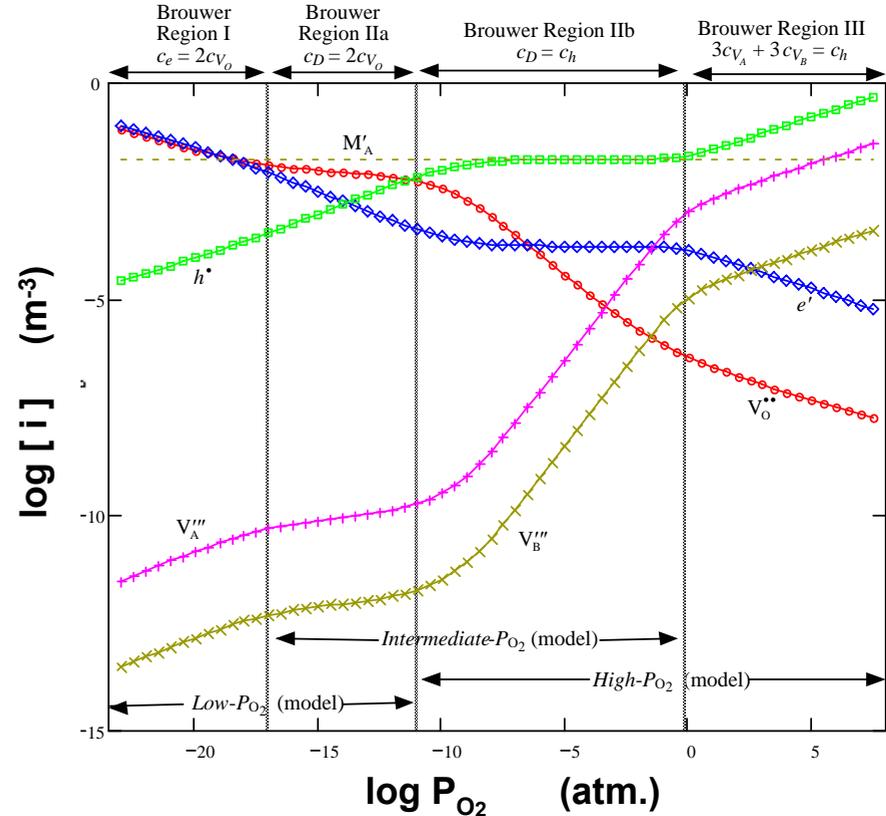
Verified experimentally
- **vs. other models[1]**
- **vs. conductivity[2]**
- **vs. OCP**
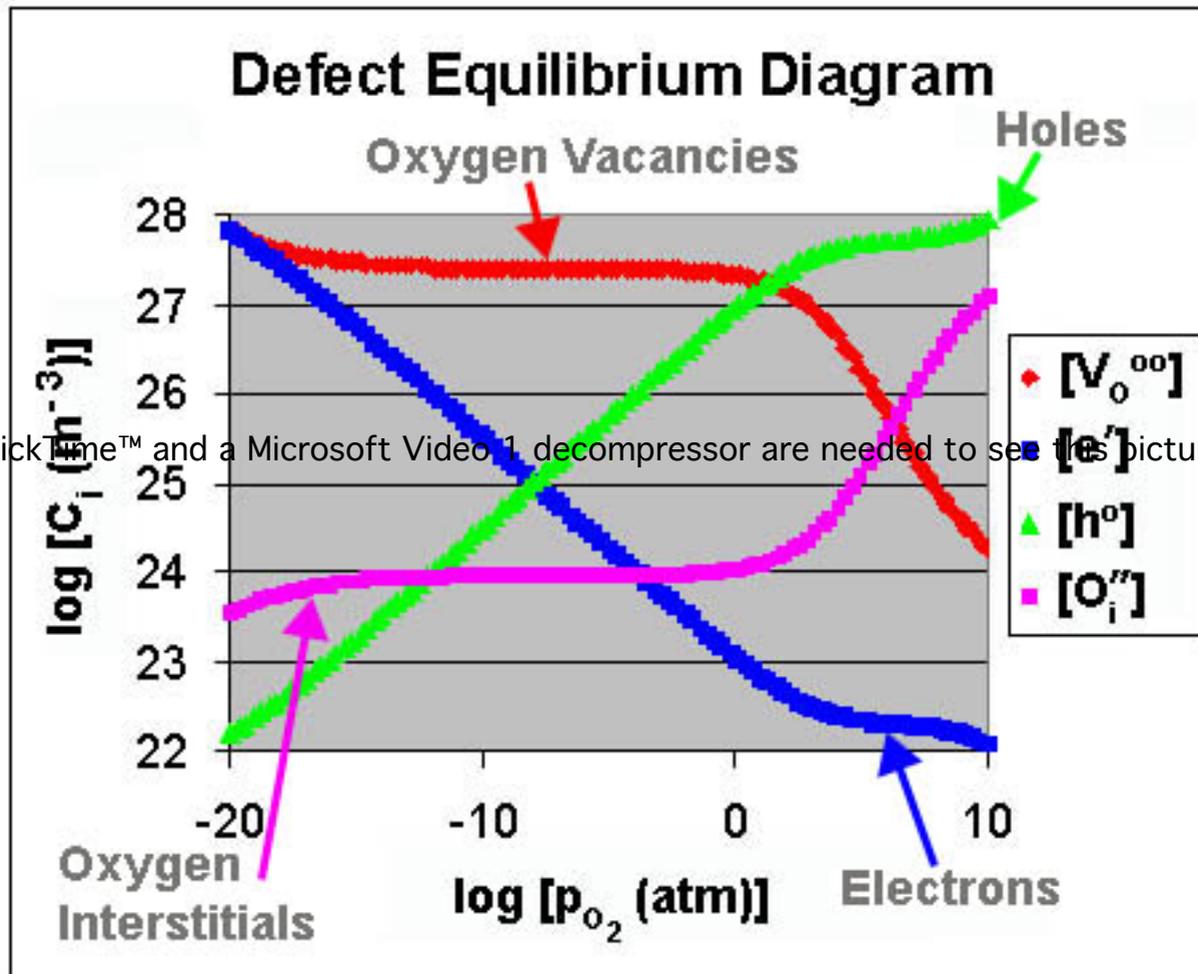
1. O. Porat and H. L. Tuller, *J. Electroceramics* **1** (1997) 42; 2. Eguchi et al, *Solid State Ionics* **52** (1992) 265.

Multiplatform C++ program
Available at www.mse.ufl.edu/~ewach

(SOFC) R_L **OR**   (ECR)

Φ_{app} J

Φ_{th} R_V J_V

$P_{O_2,0}$ (Anode) R_e J_e $P_{O_2,L}$ (Cathode)

0 L

x
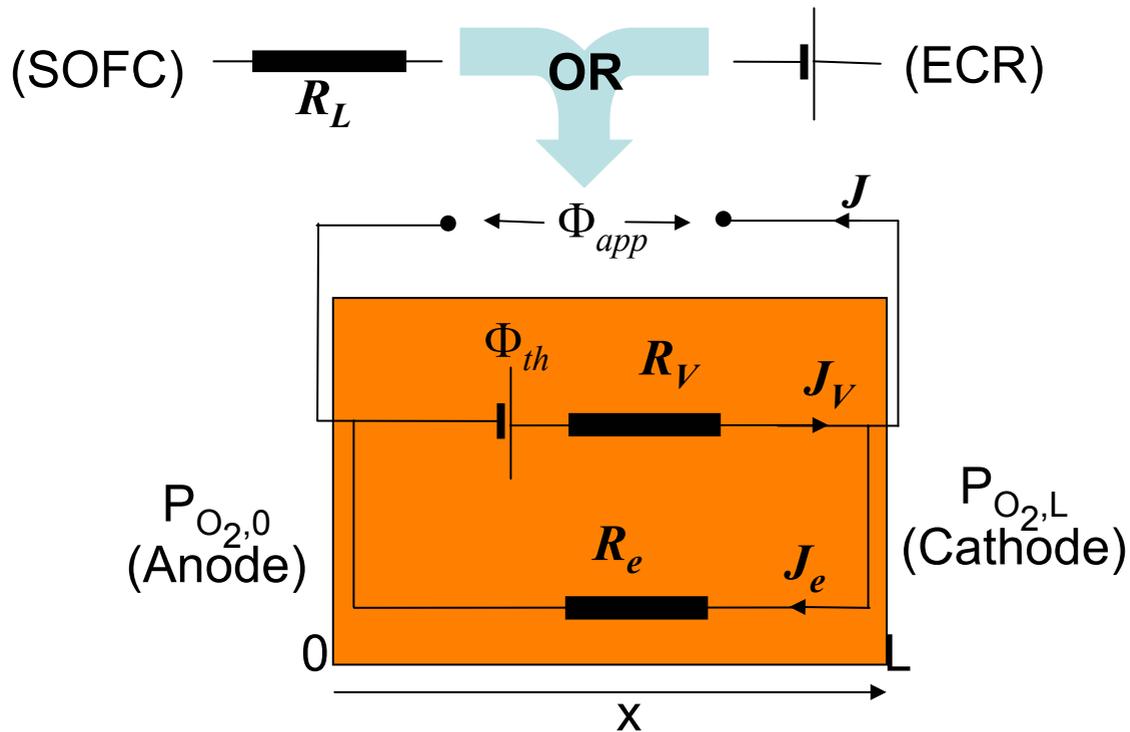
$$J = \left(\bar{t}_{ion}\Phi_{th} - \Phi_{app}\right)\bar{\sigma}_{tot} L^{-1} = \eta\,\bar{\sigma}_{tot} L^{-1}$$

overpotential, $\eta = \bar{t}_{ion}\Phi_{th} - \Phi_{app}$

FUNDAMENTAL TRANSPORT EQUATIONS & DEFINITIONS

Symbol	Definition
j	flux
J	current
c	concentration
ϕ	potential
z	charge num.
q	elec. charge
σ	conductivity
u	mobility
D	diffusivity
L	thickness
k_B	Boltz. const.
Φ_{th}	Nernst poten.
Φ_{app}	exter. potential
T	temperature

Subscripts

V	O_2 vacancies
e	electrons

Nernst-Planck

$$j_i = -D_i \nabla c_i - u_i c_i \nabla \phi$$

Current

$$J = \sum_i J_i = q \sum_i z_i j_i$$

Average conductivity

$$\overline{\sigma}_i^{-1} = L^{-1} \int_0^L \left[\sigma_i(x)\right]^{-1} \cdot dx$$

Charge neutrality

$$\sum_i z_i c_i = z_V c_V + z_A c_A + z_e c_e \approx 0$$

Local equilibrium

$$\phi_L - \phi_0 = \Delta\phi = \Phi_{app} - \Phi_{th} - k_B T \left(z_V q\right)^{-1} \ln\left(c_{V_L}/c_{V_0}\right)$$

Solved the fundamental transport equations under both:

Linear potential model (LPM) - Laplace potential distribution

Non-linear potential model (N-LPM) - Poisson potential distribution

Using both:

Fixed boundary conditions - typical in literature*

Potential dependent boundary conditions

Mathematically the N-LPM with potential dependent boundary conditions is the most accurate and most difficult

*e.g., I. Riess, *Solid State Ionics* **52** 127 (1992).

NON-LINEAR POTENTIAL MODEL $\qquad$ $\nabla J = 0$ $\qquad$ & $\qquad$ $\nabla j_i = 0$

The fact that the gradient of both the (total) current and the flux of any species is zero is used to obtain two separate (but related) differential equations.

Each differential equation is solved and the results compared to generate the model

$$\frac{\left(z_V u_e j_V - u_V j_e\right)c_V - j_V u_e c_A}{z_V\left(z_V - z_e\right)c_V - c_A} = \frac{q D_e D_V}{k_B T}\nabla c_V$$

$$\nabla^2 \phi = \lambda \nabla^2 c_V$$

$$c_V(x) - c_{V_0} - \frac{\phi(x) - \phi_0}{\lambda} = -\gamma x$$

$$c_V(x) - c_{V_0} - \frac{\left(D_V \gamma - j_V\right)c_A}{z_V\left(z_V - z_e\right)D_V \gamma} \cdot \ln \frac{z_V\left(z_V - z_e\right)D_V \gamma c_V(x) - j_V c_A}{z_V\left(z_V - z_e\right)D_V \gamma c_{V_0} - j_V c_A} = -\gamma x$$

$$\gamma = \frac{\phi_L - \phi_0}{\lambda L} - \frac{c_{V_L} - c_{V_0}}{L} \qquad\qquad \lambda = \frac{\left(z_V - z_e\right)k_B T}{z_e q c_A}$$

• The non-linearity of $\phi(x)$ increases as Φ_{ext} moves away from Φ_{oc}.

•In open-circuit conditions the Galvani potential ($\Delta\phi$) approaches zero. Hence, $\nabla^2\phi$ also goes to zero and the electric field ($\nabla\phi$) approaches linearity.
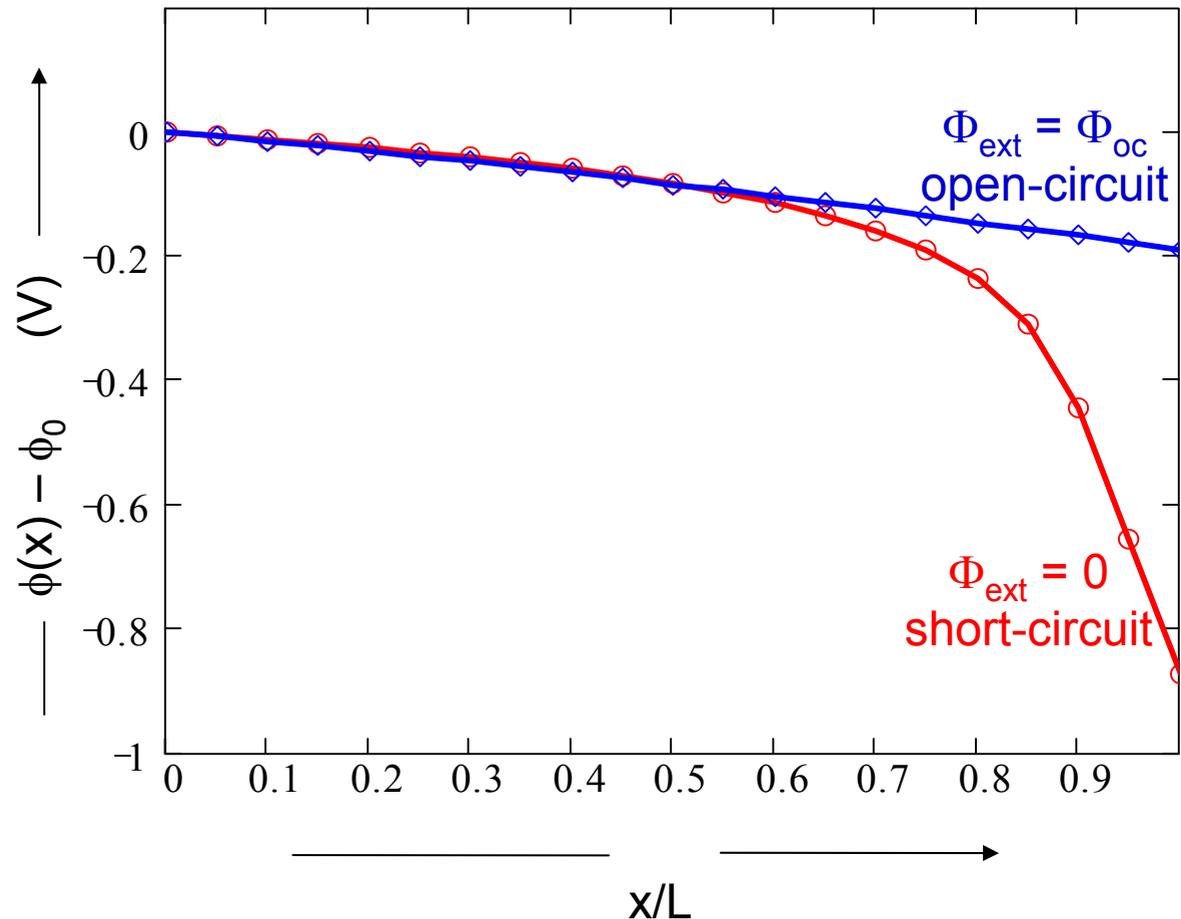
$$\phi(x) = \phi_0 - \frac{(D_V\gamma - j_V)k_B T}{z_V q D_V \gamma} \cdot \mathbf{ln}\, \frac{z_V(z_V - z_e)D_V\gamma c_V(x) - j_V c_A}{z_V(z_V - z_e)D_V\gamma c_{V_0} - j_V c_A}$$

• In *open-circuit* there is little difference between LPM and N-LPM.

• $\nabla^2\phi \propto \nabla(\nabla c_V)$, so as $\nabla c_V \to 0$, ϕ becomes a linear function of *x*.

• Significant difference between LPM and N-LPM in *short circuit* conditions where $|\nabla c_V| >> 0$.

• Concentration gradients are not confined to the "near-boundary" areas for N-LPM.
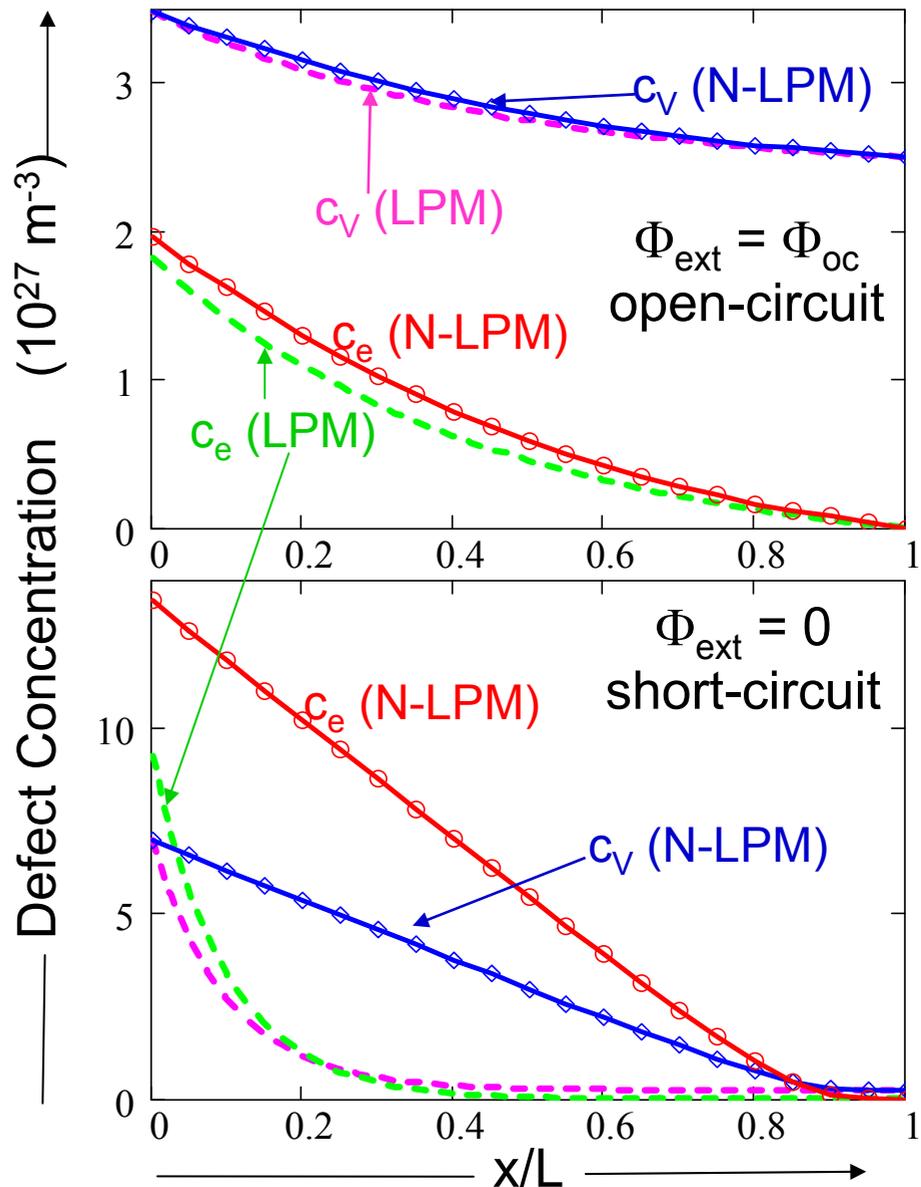
• The N-LPM doesn't "force" $\nabla c_V \approx 0$, thereby (falsely) suppressing the electron concentration. Consequently, a reduced transference number and power and current efficiency is observed.

$$j_e = j_V \frac{z_V^2}{z_e^2}\left(\frac{1}{\bar{t}_{ion}} - 1\right)\left(\frac{k_B T \ln\left(c_{e_L}/c_{e_0}\right) + z_e q \Delta\phi}{k_B T \ln\left(c_{V_L}/c_{V_0}\right) + z_V q \Delta\phi}\right)$$

$$j_V = -\frac{\left(z_V - z_e\right)q D_e D_V \gamma}{k_B T}\left[u_e - u_V \frac{z_V}{z_e^2}\left(\frac{1}{\bar{t}_{ion}} - 1\right)\left(\frac{k_B T \ln\left(c_{e_L}/c_{e_0}\right) + z_e q \Delta\phi}{k_B T \ln\left(c_{V_L}/c_{V_0}\right) + z_V q \Delta\phi}\right)\right]^{-1}$$
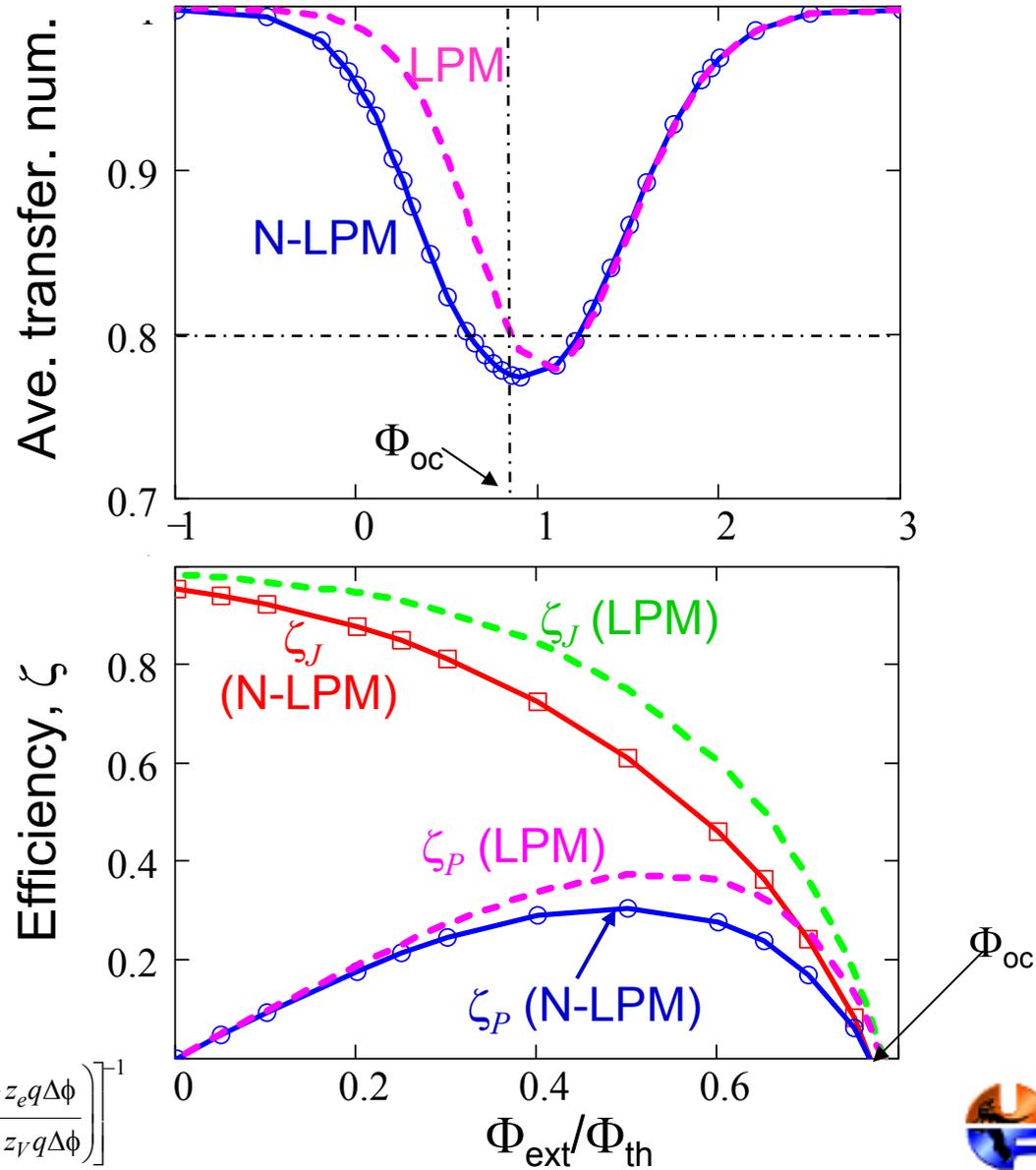
EXTENDING CONTINUUM LEVEL ELECTROCHEMICAL MODEL MODEL TO MULTILAYERED SOFC ARCHITECTURE
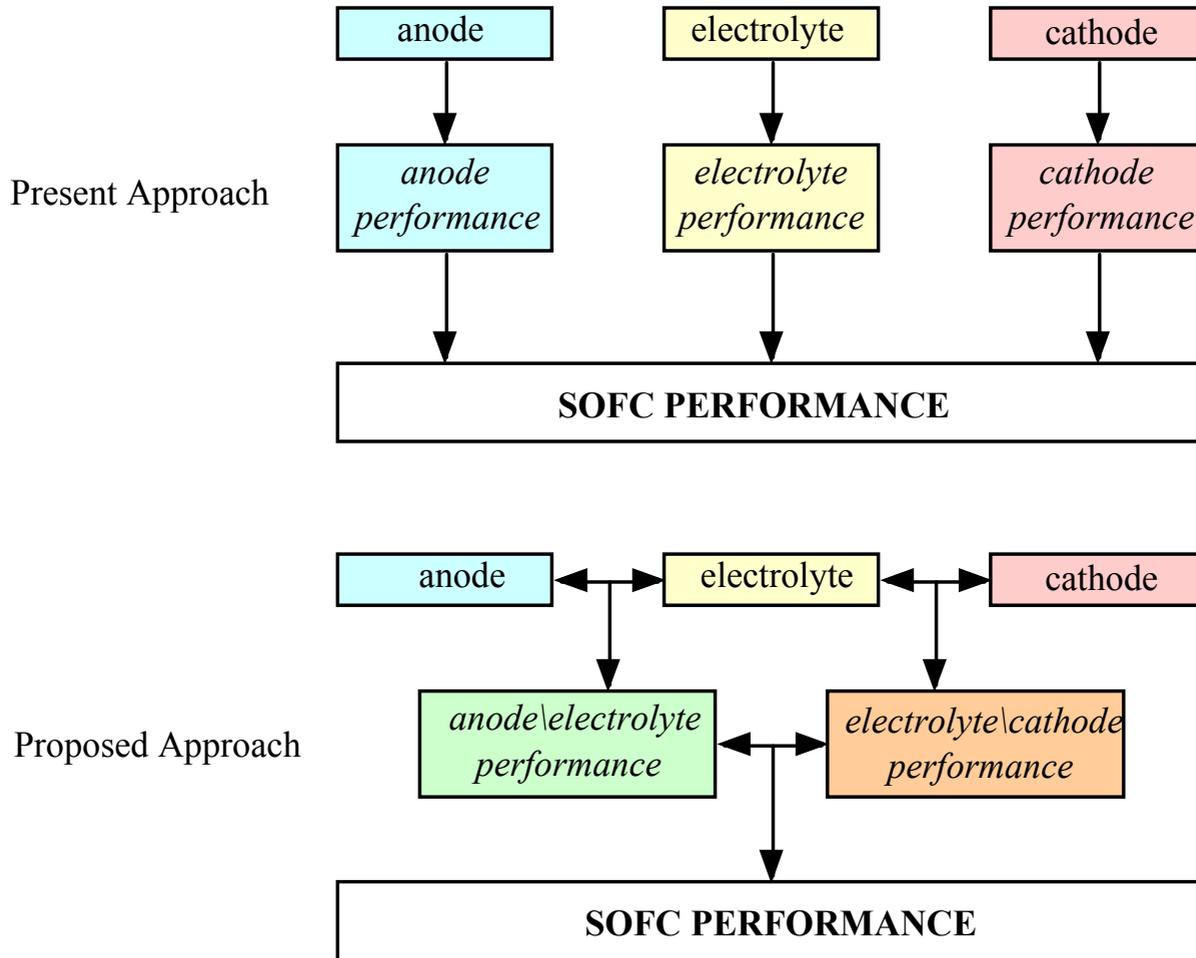
$$La_{1-y}Sr_yMnO_{3-\delta} + \delta ZrO_2 + \tfrac{3\delta}{2}O_O^\times \rightarrow La_{1-y-\delta}Sr_yMnO_{3-\delta} + \tfrac{\delta}{2}La_2Zr_2O_7 + \tfrac{3\delta}{2}V_O^{\bullet\bullet} + 3\delta e'$$

$$K \approx \left[La_2Zr_2O_7\right]^{\frac{\delta}{2}}\left[V_O^{\bullet\bullet}\right]^{\frac{3\delta}{2}}\left[e'\right]^{3\delta} = K_2\left[La_2Zr_2O_7\right]^{\frac{\delta}{2}}P_{O_2}^{-\frac{3\delta}{4}}$$

L_{YSZ} L_{LSM}

YSZ LSM

P_{O_2} Air

P_{O_2} Fuel

Interfacial P_{O_2}

P_{O_2} Profile
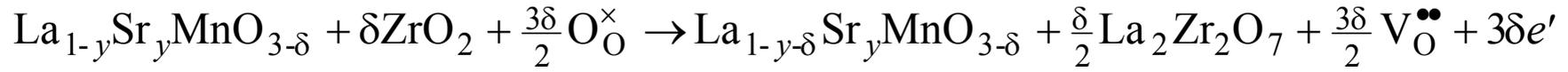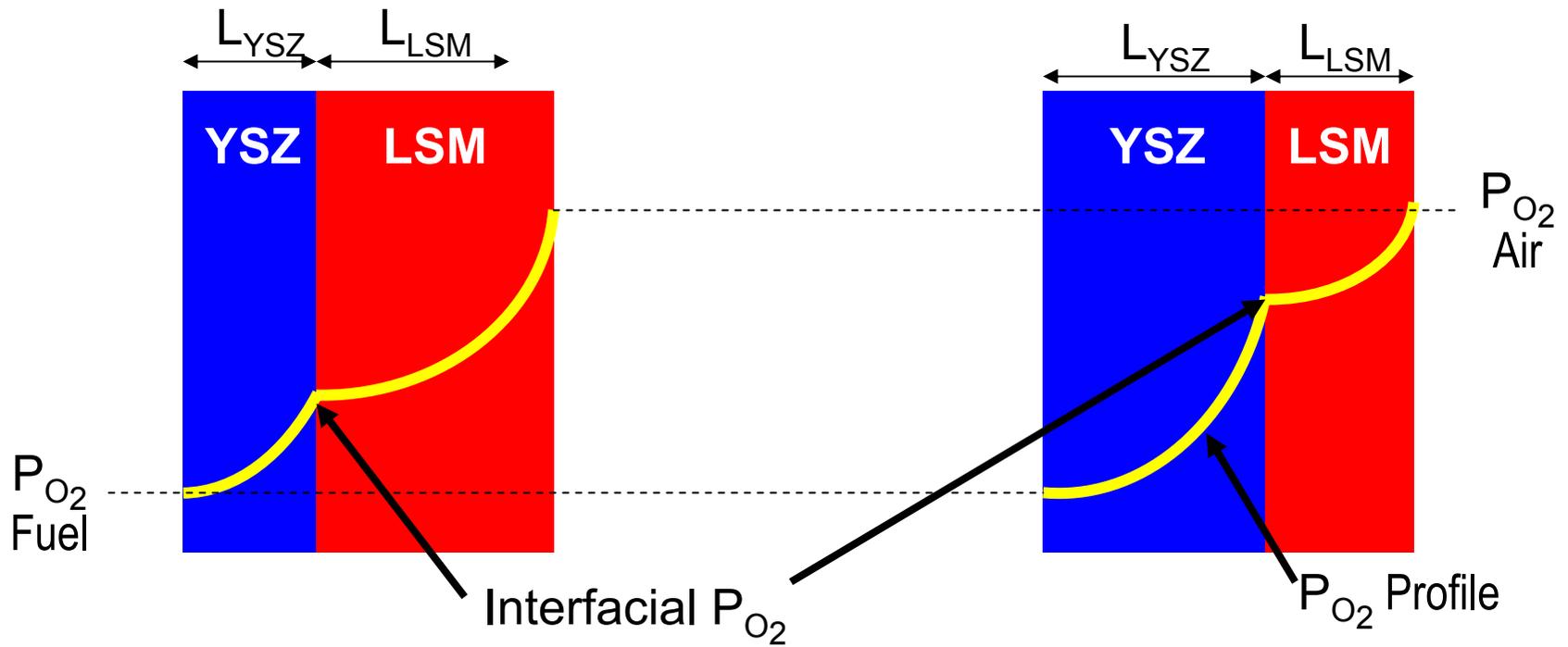
EFFECT OF ANNEAL on AC IMPEDANCE SPECTRA of LSM/YSZ/LSM CELLS
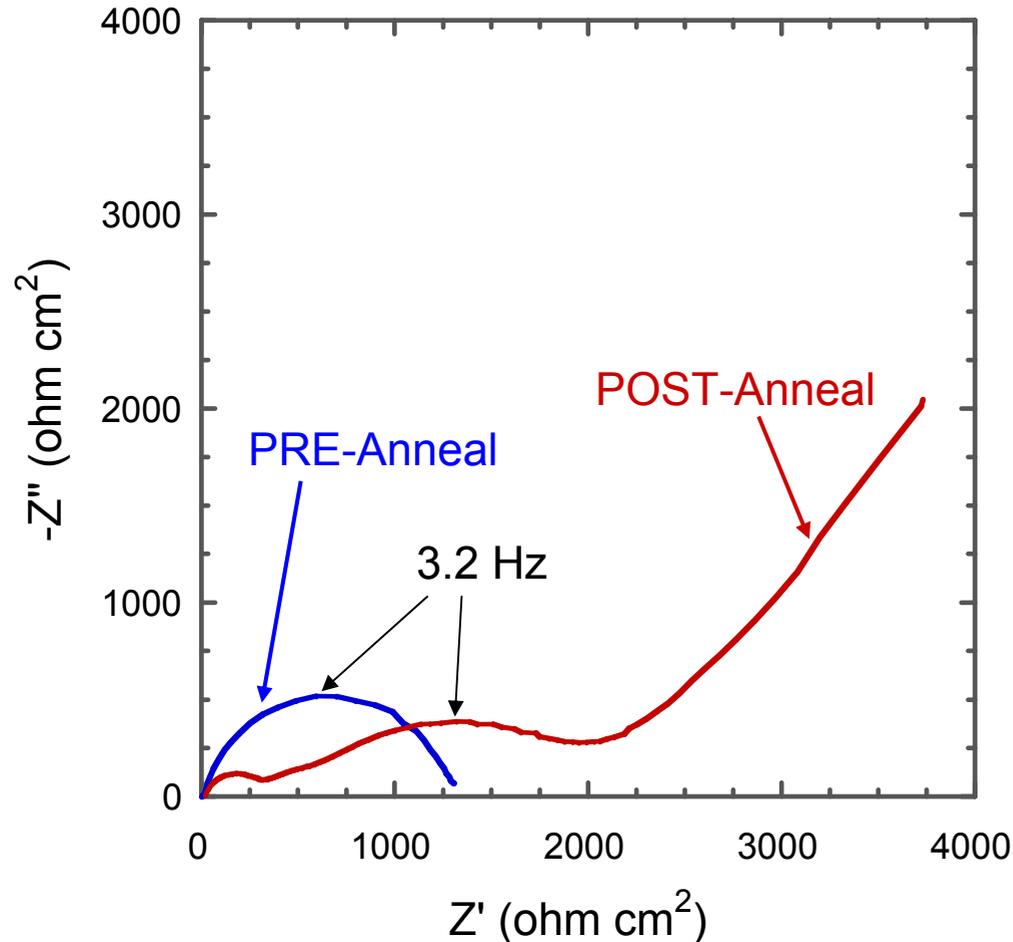
- Annealed at 1400 °C for 48 hours

- Presence of 3.2 Hz resonant frequency in pre- and post-anneal samples indicate that one transport phenomena remains the same

- Additional post-anneal features due to formation of interfacial phase(s)

- Formation of additional phase to be compared with CLEM predictions of interfacial P_{O2}

- Time dependence of growth of additional phase to be compared with transient CLEM

Samples supplied by NexTech
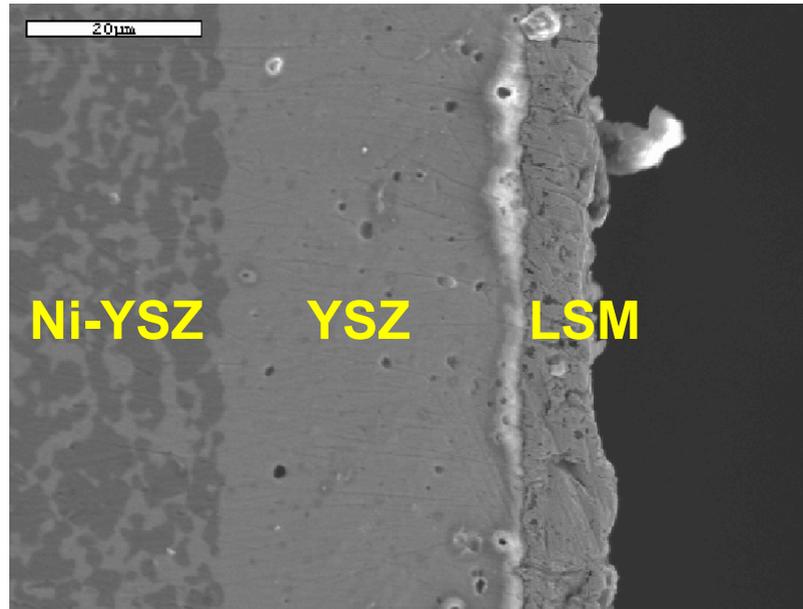
$$R \equiv f(P_{O2}, c_i, \Phi_{ext}, K)$$

$$C \equiv f(P_{O2}, c_i, \Phi_{ext}, K)$$

Ni-YSZ   **YSZ**   **LSM**

C_{bulk} $C_{surface}$ C_{bulk} $C_{g\text{-}b}$ C_{bulk} $C_{surface}$

R_{bulk} $R_{surface}$ R_{bulk} $R_{grain\text{-}boundary}$ R_{bulk} $R_{surface}$
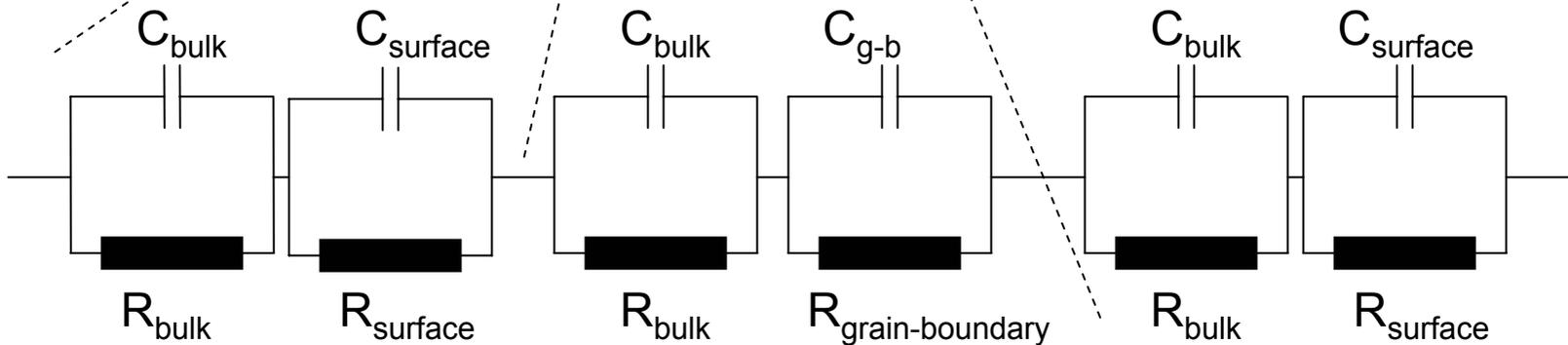
RESOLVING the AC IMPEDANCE SPECTRA

"Raw" impedance spectra

400 ¡C

-Z" (ohm cm^2)

Z' (ohm cm^2)

400 ¡C

-Z" (ohm cm^2)

Z' (ohm cm^2)

Samples supplied by NexTech

Table 1. Electrode resistance, R, capacitance, C and time constant, τ (= RC) from EIS.

	Test Temperature (°C)	$R_{electrode}$ (Ω)	$C_{electrode}$ (μF)	$\tau_{elecrode}$ (s)	$1/\tau_{elecrode}$ (Hz)
	500	50400	23.6	1.19	0.840
	700	820	51.5	4.22×10^{-2}	23.7
LSM/YSZ	800	131	71.2	1.02×10^{-2}	98.0
	900	22.1	115	2.54×10^{-3}	394
	700	438	208	9.11×10^{-2}	11.0
LSF/YSZ	800	134	165	2.21×10^{-2}	45.2
	900	1.24	11100	1.37×10^{-2}	73.0

• Choice of electrode material and operating temperature influence susceptibility to 60Hz transients

Samples supplied by NexTech

TRANSIENT TRANSPORT MODEL FOR ZIRCONIA

Nernst-Planck flux equation

$$j_i = -D_i \nabla c_i - u_i c_i \nabla \phi$$

Material balance equation

$$\frac{\partial c_i}{\partial t} = -\nabla j_i$$

Current equation

$$J = q \sum_i z_i j_i$$

Equations for flux, material balance, current and charge neutrality are manipulated to obtain expressions for the rate of change of defect concentration.

$$\frac{\partial c_V}{\partial t} = \frac{D_e D_V}{z_e D_e - z_V D_V} \left[(z_e - z_V) \nabla^2 c_V + z_e c_A \frac{q}{k_B T} \nabla^2 \phi \right]$$

$$\frac{\partial c_e}{\partial t} = \frac{D_e D_V}{z_e D_e - z_V D_V} \left[(z_e - z_V) \nabla^2 c_e + z_e z_V c_A \frac{q}{k_B T} \nabla^2 \phi \right]$$

And an expression for the electric field as a function of defect concentrations.

$$\nabla \phi = -\frac{J + (z_V q D_V \nabla c_V + z_e q D_e \nabla c_e)}{q(z_V u_V c_V + z_e u_e c_e)}$$

TRANSIENT EFFECTS ON DEFECT CONCENTRATION - using Fourier series

CASE 1: Introduction of a P_{O_2} gradient

Here we consider what happens when a zirconia electrolyte is first placed into a P_{O_2} gradient.

$$c_e(x,t) = \sum_{n=1}^{\infty} \frac{2\left((-1)^n c_{e,L}^{\infty} - c_{e,0}^{\infty} + c_e^0\right)}{n\pi} e^{-\alpha^2\left(\frac{n\pi}{L}\right)^2 t} \sin\frac{n\pi}{L}x + \frac{c_{e,L}^{\infty} - c_{e,0}^{\infty}}{L}x + c_{e,0}^{\infty}$$

$$\phi(x,t) = \frac{2D_e}{u_V c_A} \sum_{n=1}^{\infty} \frac{(-1)^n c_{e,L}^{\infty} - c_{e,0}^{\infty} + c_e^0}{n\pi} e^{-\alpha^2\left(\frac{n\pi}{L}\right)^2 t} \sin\frac{n\pi}{L}x + \frac{\phi_L^{\infty} - \phi_0^{\infty}}{L}x + \phi_0^{\infty}$$

CASE 2: Changing the load resistance and/the applied potential.

Here we consider what happens when the load resistance or an applied potential is changed for a zirconia electrolyte already operating in a P_{O_2} gradient

$$c_e(x,t) = \sum_{n=1}^{\infty} \frac{2\left[(-1)^{n-1}\left(c_{e,L}^0 - c_{e,L}^{\infty}\right) + \left(c_{e,0}^0 - c_{e,0}^{\infty}\right)\right]}{n\pi} e^{-\alpha^2\left(\frac{n\pi}{L}\right)^2 t} \sin\frac{n\pi}{L}x$$

$$+ \frac{c_{e,L}^{\infty} - c_{e,0}^{\infty}}{L}x + c_{e,0}^{\infty}$$

$$\phi(x,t) = \frac{D_e}{u_V c_A} c_e(x,t)$$

TRANSIENT EFFECTS ON DEFECT CONCENTRATION

CASE 1
Introduction of a P_{O_2} gradient

CASE 2
Changing the P_{O_2} gradient/applied potential/load resistance
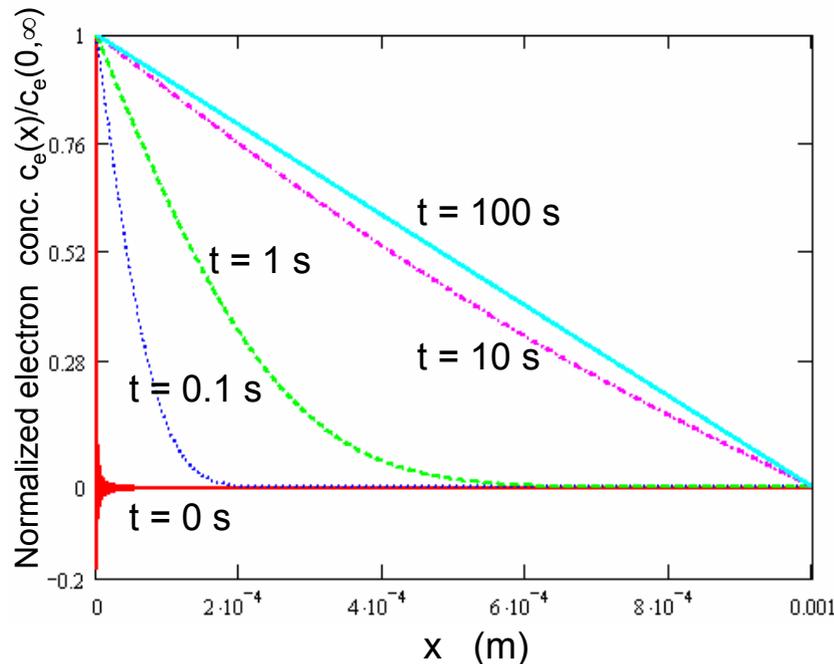
Before the zirconia electrolyte is introduced to a P_{O_2} gradient (i.e., at t = 0), the concentration distribution is flat. After the P_{O_2} gradient is introduced, a new concentration distribution gradually established.
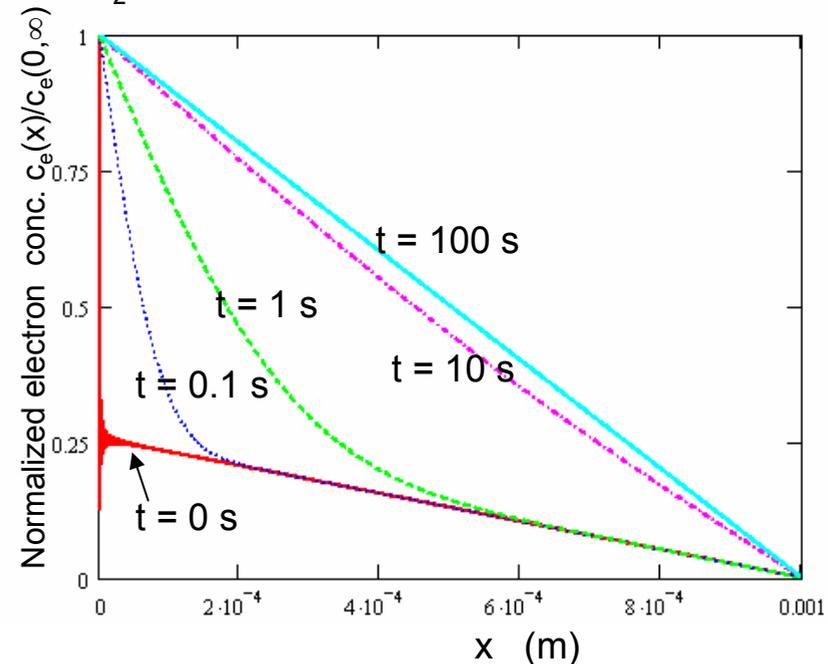
After the boundary concentrations are perturbed a new concentration distribution gradually established.

For the above processes, the time constant, τ,
• $\tau \propto 1/L$ (steady-state achieved more rapidly for thinner electrolytes)
• $\tau \propto D_e$ (rapid electron diffusion helps system to reach steady-state

CASE 1: Introduction of a P_{O_2} gradient

time

c_e (m^{-3})

$4 \cdot 10^{24}$

$2 \cdot 10^{24}$

100 80 60 40 20

0   1   2   3   4

C

c_e (m^{-3})

10^{24}

10^{24}

0   1   2   3   4

0 20 40 60 80 100

C

x

CASE 1 + Sinusoidal variation
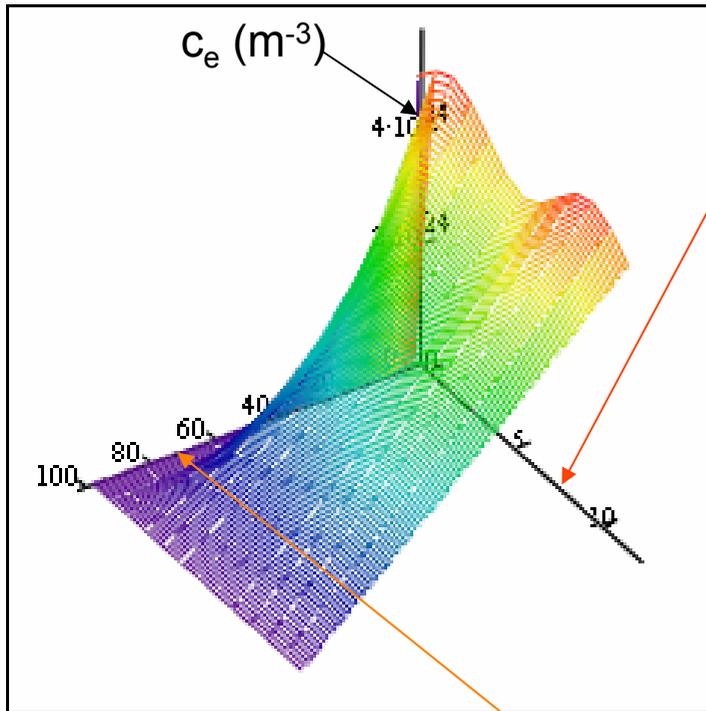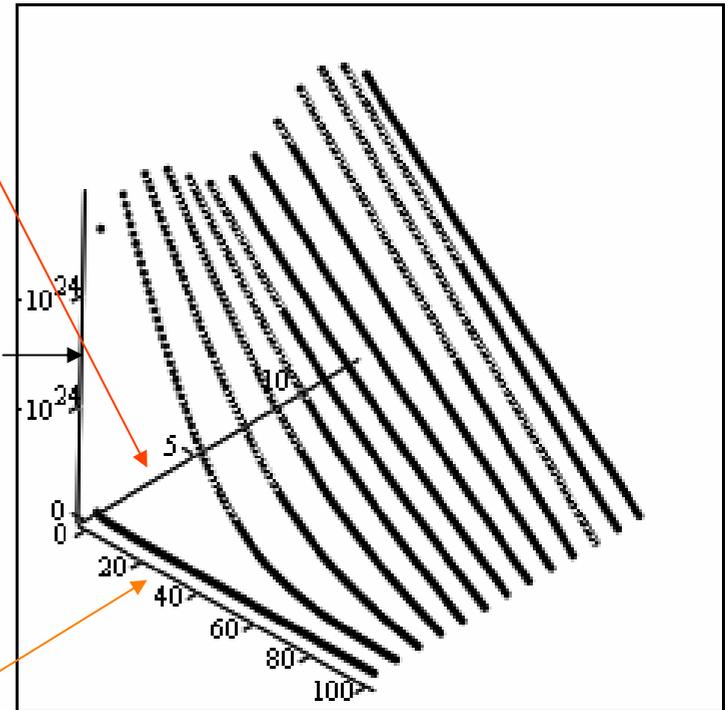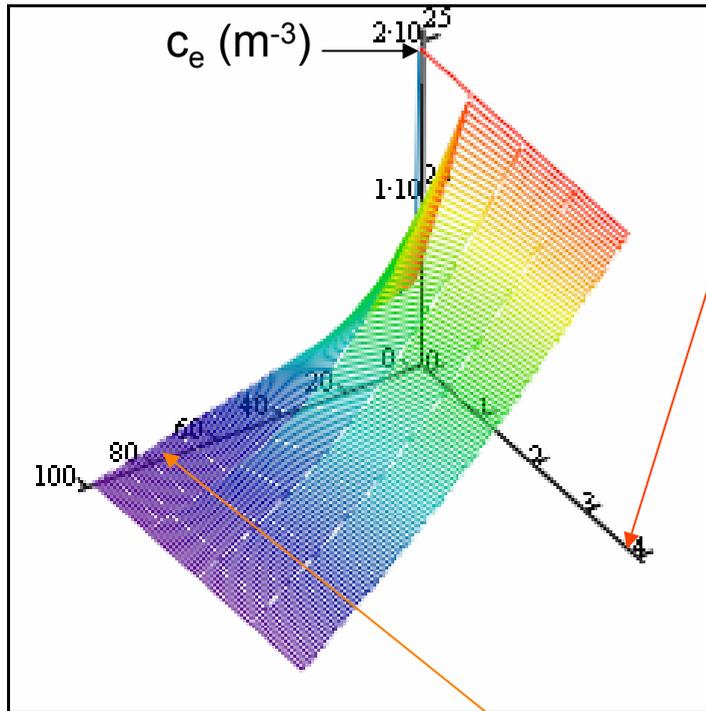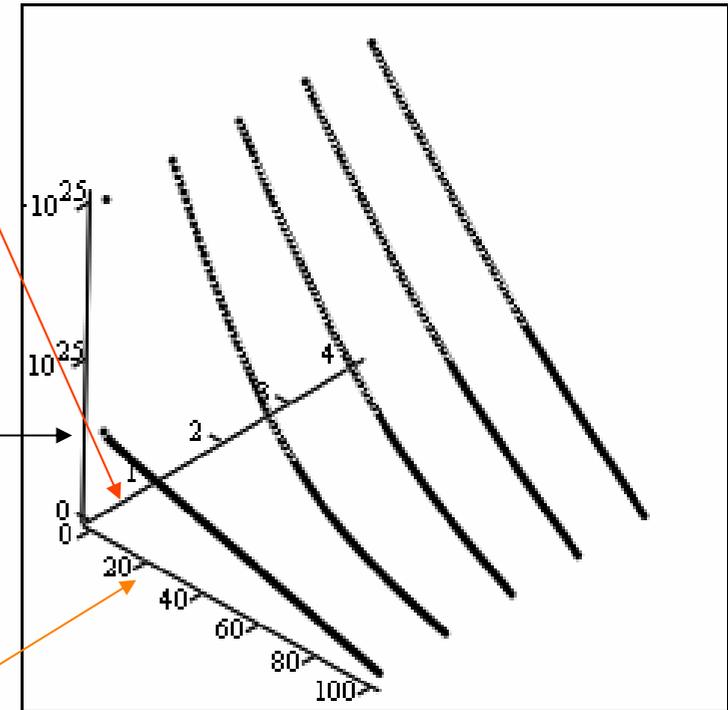
CASE 2: Changing the P_{O_2} gradient/applied potential/load resistance

CASE 2 + Square-wave variation
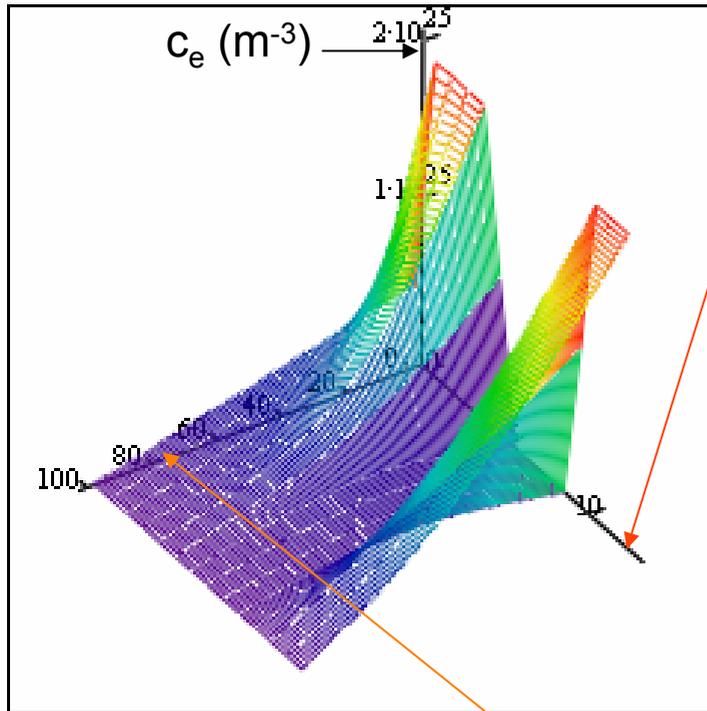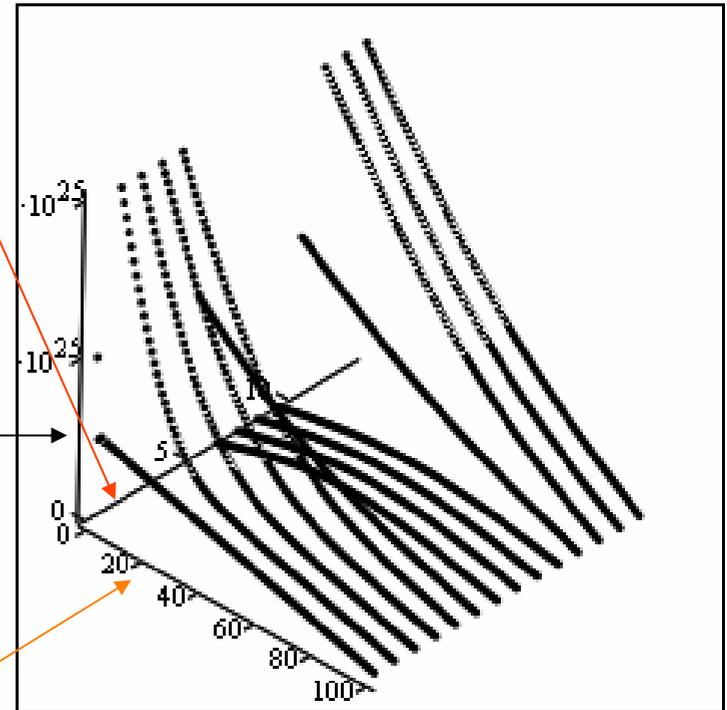
Case 2 Changing the P_{O_2} gradient/applied potential/load resistance
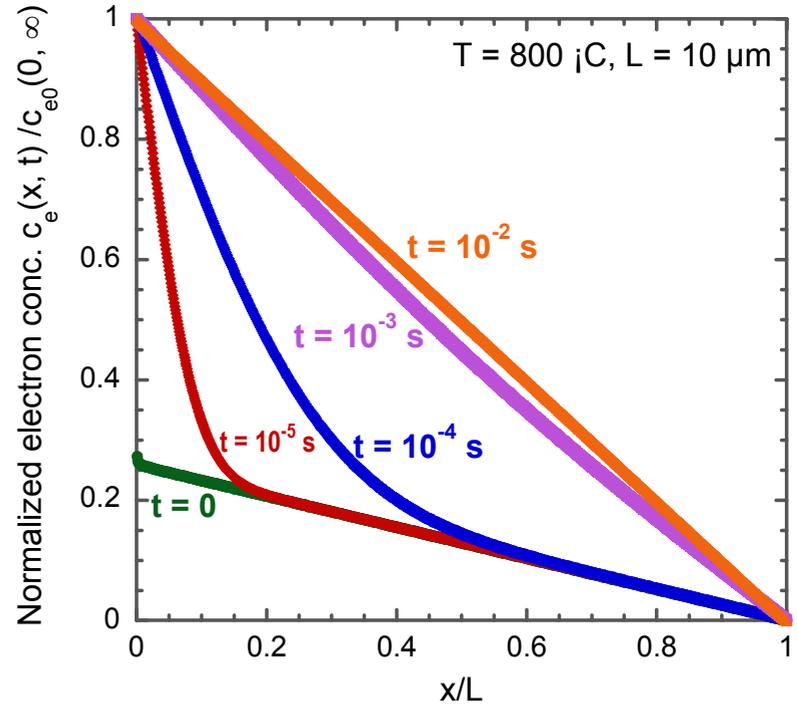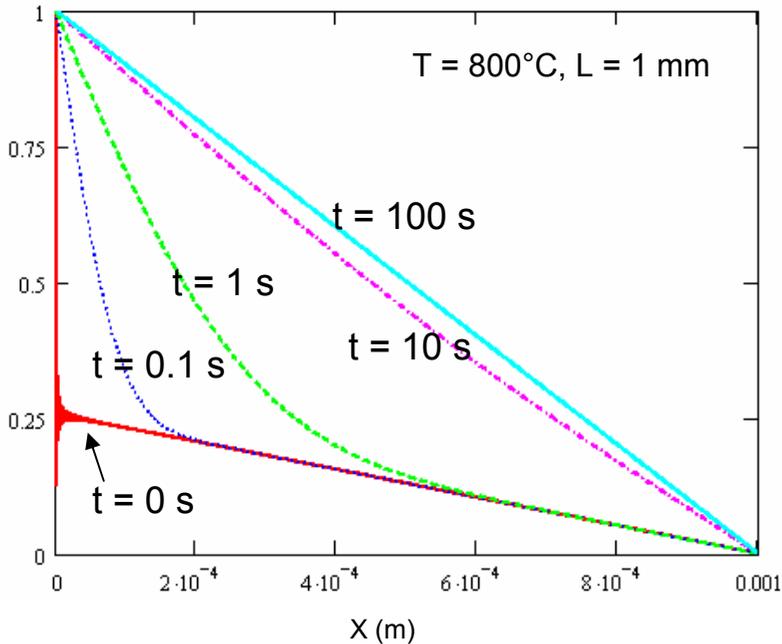
- **Importance of transients depends on layer thickness**

$$E_{bond} \approx (1 - mn^{-1})Ba^{-m}$$

*where B, n and m are empirically determined constants and

a is the lattice parameter.

also

$$Y \sim a^{-(m+3)} \quad \text{and} \quad K_{IC} \sim Y^{1/2}a^{-3/2}$$

&

$$a \sim c_V$$

$$Y(x)/Y^\circ \approx \left(\sqrt[m+3]{Y^\circ} b_1 c_V(x) + 1 \right)^{-(m+3)}$$

$$K_{IC}(x)/K_{IC}^\circ \approx \left(\sqrt[m+6]{\left(K_{IC}^\circ\right)^2} b_2 c_V(x) + 1 \right)^{-\frac{m+6}{2}}$$

* M. Barsoum, in Fundamentals of Ceramics (McGraw-Hill, 1977).

Short Circuit

Open Circuit

$(Y^*)^{1/4}b_1 = 10^{-30}$ m^3

$(Y^*)^{1/4}b_1 = 2\times10^{-30}$ m^3

$Y(x)=Y^*[(Y^*)^{1/4}b_1 c_V(x)+1]^{-4}$

$(K_{IC}^*)^{2/7}b_2 = 3\times10^{-30}$ m^3

$(K_{IC}^*)^{2/7}b_2 = 6\times10^{-30}$ m^3

$K_{IC}(x)=K_{IC}^*[(K_{IC}^*)^{2/7}b_2 c_V(x)+1]^{-3.5}$

x/L

x/L
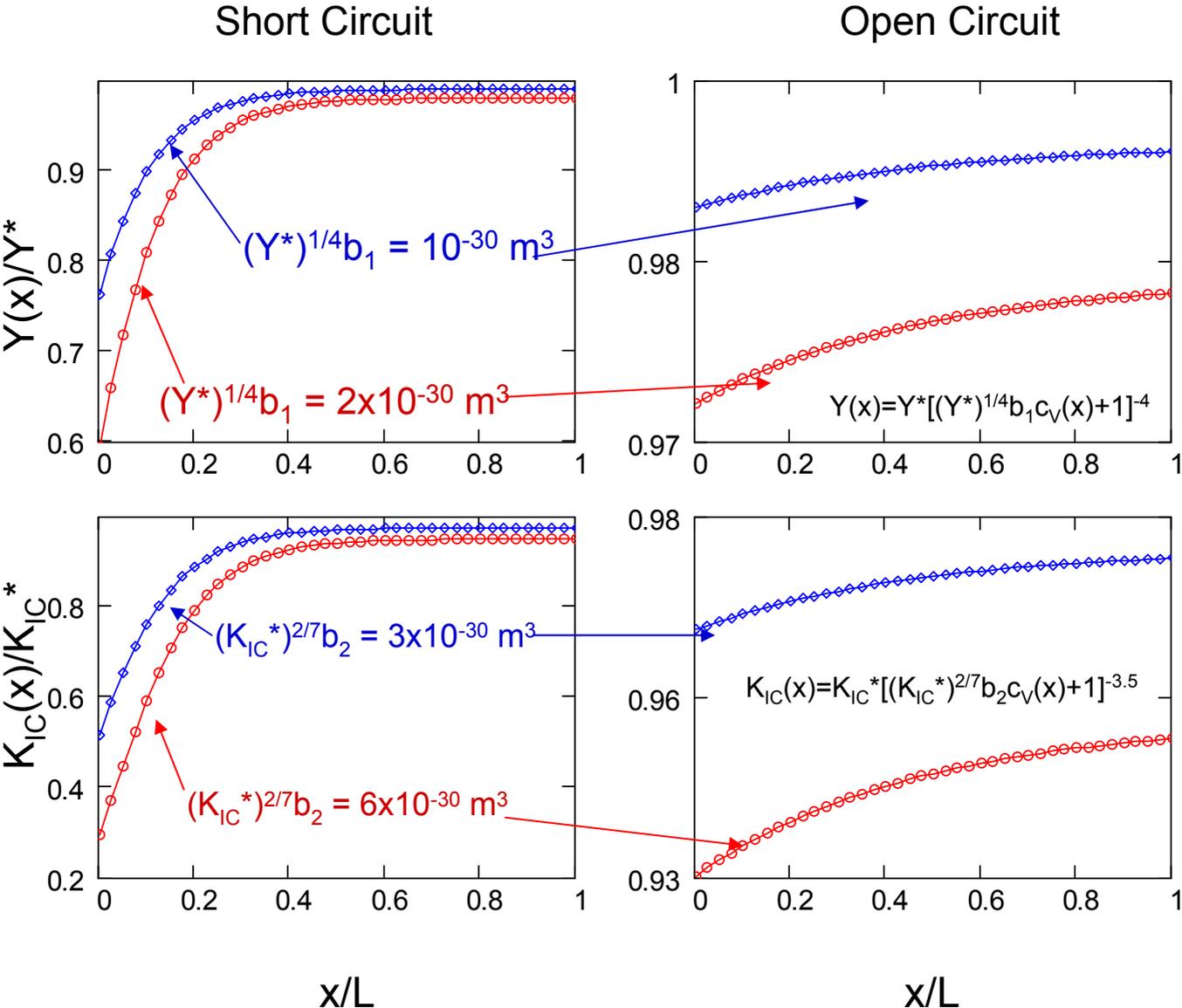
- Vacancy concentration as a function of P_{O_2} (Cahn Microbalance)

$$c_v = f(T, P_{O_2}) \rightarrow K(T)$$

- Thermal expansion as a function of P_{O_2} (THETA Dilatometer)

$$\Delta L \sim \Delta c_v = f(T, P_{O_2})$$
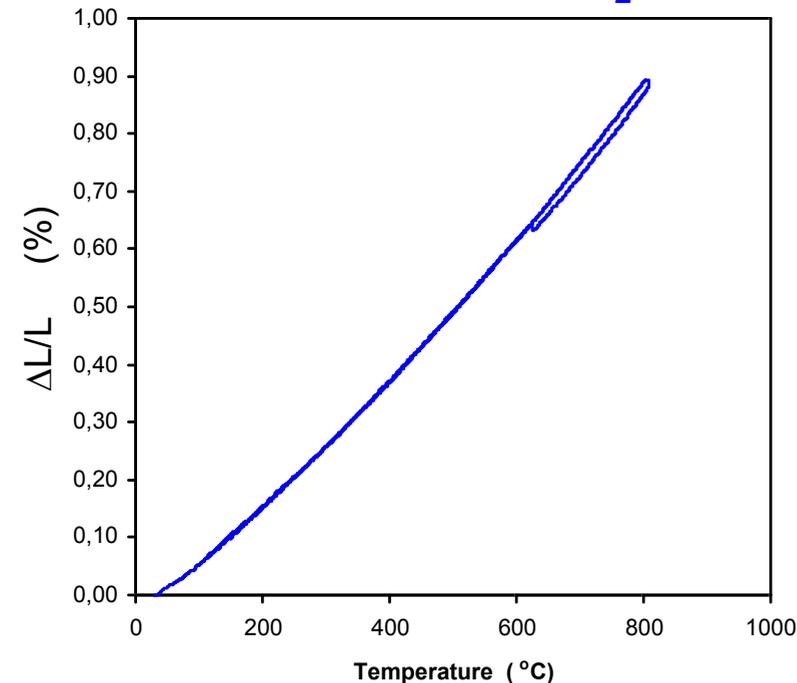
- Measured with Theta® dilatometer
- Initial length 12.1 mm CeO_2
- CTE / 10^{-6} ^{o}C^{-1}

Temp	CTEx 10^{-6}
700°C	12.2 ^{o}C^{-1}
750°C	12.7 ^{o}C^{-1}
800°C	13.2 ^{o}C^{-1}
800°C*	13.05 ^{o}C^{-1}

*Sameshima *et al.* J.Cer. Soc. of Japan **110** (2002)

- Bulk Elastic Moduli and Fracture Toughness (Triboindenter)

$$Y \text{ and } K_{IC} \sim f(C_v) = f(T, P_{O_2})$$

- Bulk Elastic Moduli (Resonant Ultrasound) at high temperature as a function of P_{O_2}
  - E. Lara-Curzio, ORNL
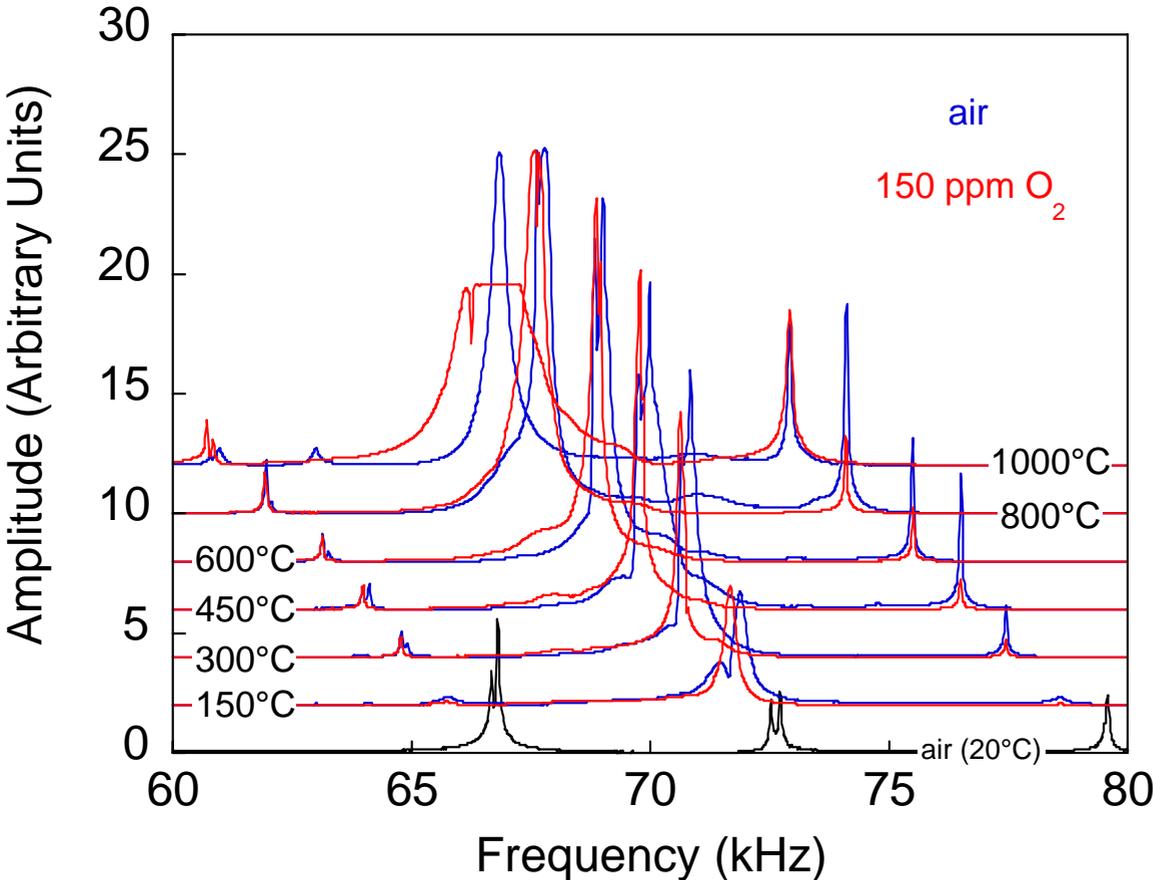
Broadening of peaks and shift to lower frequency indicate weaker bonds and lower modulus under low P_{O2}, consistent with model predictions.

$$Y \sim f(C_v) = f(T, P_{O_2})$$

Evolution of resonant ultrasound spectrum as a function of temperature for tests carried out in air (blue peaks) or in an environment with 150 ppm of O_2 (red peaks).

More than 40 peaks were used to estimate the magnitude of the elastic properties.

• Elastic Moduli and Fracture Toughness (MTS) at high temperature and as a function of P_{O_2}

For polycrystalline samples

Y and $K_{IC} \sim f(C_v) = f(T, P_{O_2})$

What is affect of microstructure?

CONCLUSIONS

We have developed a continuum level electrochemical model from which we can obtain

1. Continuous equations relating defect concentration to oxygen potential

2. Assumption free equations for the:

   - Spatial distribution of ionic and electronic defects

   - Transport properties

   - Power and current efficiency of SOFC electrolytes and MIECs

3. Thermo-chemical stability

4. Thermo-mechanical properties

5. Time evolution of the transport properties of oxide ion conducting materials.

We have prepared a packaged software for defect equilibria calculations (available on the web) and will shortly include electrochemical performance and deliver to NETL, PNNL and ORNL (and any interested SECA teams).

We have initiated experimental work to obtain thermodynamic, electrochemical and mechanical property constants, and validate model.